WINDOWS IN A NON-AUTONOMOUS CIRCUIT WITH SYMMETRY

Miyoshi T., *Sekikawa M.*†, *Sato T.*‡, *Inaba N.*§ and *Nishio Y.*¶

*†‡§ Faculty of Engineering, Utsunomiya University, Utsunomiya, 321-8585 Japan
¶Faculty of Engineering, Tokushima University, Tokushima, 770-8506 Japan

ABSTRACT

Symmetric structure exists in many chaos-generating circuits. In those circuits, interesting bifurcation phenomena based on the symmetry of circuits, such as symmetry recovering, symmetry breaking and so on, are observed. In the present study, two types of interesting windows are observed in a circuit with symmetry which we propose. This circuit has a pair of diodes. We consider the case in which the pair of diodes operates as a pair of ideal switches. In this case, the Poincaré map can be derived rigorously as a one-dimensional map. We prove that a countably infinite number of two types of windows are generated alternately by applying the theorem written in our paper[1] to the one-dimensional map.

1. INTRODUCTION

Symmetric structure exists in many chaos-generating circuits. Chua's circuit is an example. The governing equation is invariant against the transformation $(x, y, z) \rightarrow (-x, -y, -z)$ because the characteristic of the nonlinear element is symmetric with respect to the origin[2]. In circuits having such symmetry, interesting bifurcation phenomena such as symmetry recovering and symmetry breaking occur.

We proposed a three-dimensional autonomous circuit whose governing equation is invariant against the transformation $(x, y, z) \rightarrow (-x, -y, -z)$ and analyzed generated windows[1]. A window is a periodic phase surrounded by chaotic phases. By analyzing the Poincaré map, it was clarified that certain two types of windows are generated by the target circuit. Furthermore, it was clarified theoretically that a countably infinite number of the two types of windows are generated alternately.

On the other hand, symmetric structure exists also in non-autonomous systems such as Duffing equation and a forced Rayleigh equation. They are invariant against the transformation $(t, x, y) \rightarrow (t+2\pi/\omega, -x, -y)$, where ω denotes the angular frequency of the external force.

In the present study, we analyze windows which are generated by a forced Rayleigh circuit having a pair of diodes. By numerical calculation, it is clarified that the circuit generates two types of windows.

*E-mail: miyoshi@every.is.utsunomiya-u.ac.jp
†E-mail: moosk@every.is.utsunomiya-u.ac.jp
‡E-mail: teching@every.is.utsunomiya-u.ac.jp
§E-mail: inaba@is.utsunomiya-u.ac.jp

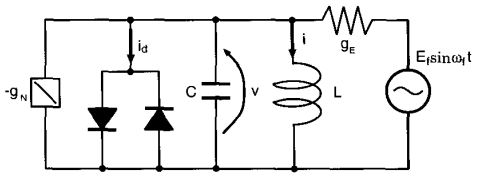

Figure 1: Target circuit.

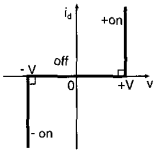

Figure 2: v-i_d characteristic of ideal diode pair.

One type is a window in which symmetry breaking bifurcation occurs. The other is a window where the shape of the orbit stays unsymmetric with respect to the origin. Those are the same as the autonomous circuit mentioned above.

The circuit is analyzed assuming the pair of diodes to be a pair of ideal switches. In the domain where one of the diodes is on, the governing equation is degenerated to a one-dimensional equation because of the assumption. Therefore the Poincaré map is derived rigorously as a one-dimensional map. By applying the theorem written in our paper[1], it is proved that a countably infinite number of the two types of windows are generated alternately.

2. TARGET CIRCUIT

The target circuit is shown in Fig. 1, where $-g_N$, g_E, v, i, i_d, E, and ω_f denote linear negative conductance, positive conductance, the voltage across the capacitor C, the current through the inductor L, the current through the pair of diodes, the amplitude of the external force, and the angular frequency of the external force, respectively. We approximate that the v-i characteristic of the pair of diodes is shown in Fig. 2. Let us change variables as follows.

$$\tau = \frac{t}{\sqrt{LC}}, \quad x = \frac{i}{V}\sqrt{\frac{L}{C}}, \quad \delta = \frac{g_N - g_E}{2}\sqrt{\frac{L}{C}},$$

0-7803-7057-0/01/$10.00 ©2001 IEEE.

$$E = \frac{g_E E_f}{V}\sqrt{\frac{L}{C}}, \quad \omega = \omega_f\sqrt{LC}, \quad \bullet = \frac{d}{d\tau}. \quad (1)$$

We obtain the following governing equations. As Fig. 2 shows, the branch where one diode is on is denoted by $+on$ and the other $-on$.

$$\begin{cases} +on: & \dot{x} = 1, \\ off: & \ddot{x} - 2\delta\dot{x} + x = E\sin\omega\tau, \\ -on: & \dot{x} = -1. \end{cases} \quad (2)$$

While the diode pair is $+on$ ($-on$), $\dot{x}$ equals 1 (-1) because the voltage across the capacitor is constrained by the threshold voltage of the diode. Note that the dimension of the equation is degenerated to one on the branches $+on$ and $-on$. The solution of Eq. (2) is connected by the following condition.

$$\begin{cases} off \to +on: & \dot{x} = 1, \\ +on \to off: & x = 2\delta + E\sin\omega\tau, \\ off \to -on: & \dot{x} = -1, \\ -on \to off: & x = -2\delta + E\sin\omega\tau. \end{cases} \quad (3)$$

Let us call Eqs. (2) and (3) the constrained equations.

3. POINCARÉ MAP

While the diode pair is $+on$ ($-on$), the dimension of the constrained equation is one. Therefore the Poincaré map is derived as a one-dimensional map. We use some symbols to define the Poincaré map. D^+, D, and D^- denote three subsets of τ-x-$\dot{x}$ space where the diode pair is $+on$, off, and $-on$, respectively, as follows.

$$\begin{aligned} D^+ &= \{(\tau, x, \dot{x}) \mid \dot{x} = 1\}, \\ D &= \{(\tau, x, \dot{x}) \mid |\dot{x}| < 1\}, \\ D^- &= \{(\tau, x, \dot{x}) \mid \dot{x} = 1\}. \end{aligned} \quad (4)$$

We treat the case in which $0 < \delta < 1$. In that case, eigenvalues of the constrained equations in the domain D are conjugate complex numbers $\delta \pm j\gamma$ ($\gamma = \sqrt{1-\delta^2}$). Because Eq. (2) is piecewise linear, the solution is derived analytically in each domain. It is described as follows.

$$\begin{pmatrix} x(\tau) \\ \dot{x}(\tau) \end{pmatrix} = \begin{pmatrix} \phi(\tau, P, \lambda) \\ \dot{\phi}(\tau, P, \lambda) \end{pmatrix}, \quad (5)$$

where $P = (\tau_0, x_0, \dot{x}_0)$ denote the initial condition and $\lambda = (\delta, \omega, E)$. Let each solution in each domain where the diode pair is $+on$, off, and $-on$ be denoted by $(\phi_{+on} \quad \dot{\phi}_{+on})^T$, $(\phi_{off} \quad \dot{\phi}_{off})^T$, and $(\phi_{-on} \quad \dot{\phi}_{-on})^T$, respectively. Each solution is derived analytically. Its formula is omitted owing to limited space.

Let us define curved lines C^+ and C^- as follows.

$$\begin{aligned} C^+ &= \{(\tau, x, \dot{x}) \mid x = 2\delta + E\sin\omega\tau, \dot{x} = 1\}, \\ C^- &= \{(\tau, x, \dot{x}) \mid x = -2\delta + E\sin\omega\tau, \dot{x} = -1\}. \end{aligned} \quad (6)$$

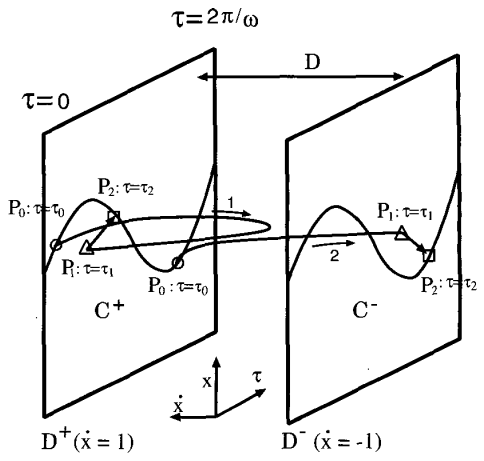

Figure 3: Orbits.

C^+ and C^- describe the connection position determined by Eq. (3). C^+ corresponds to the $+on \to off$ connection and is on the plane D^+. C^- corresponds to the $-on \to off$ connection and is on the plane D^-.

Fig. 3 shows the structure of the vector field of orbits. In the figure, two examples of orbits are drawn. We treat the case in which $0 < \omega E < 1$. Let us consider the solutions whose initial points are on the line C^+. The solutions whose initial points are on the line C^+ are classified into the following two cases.

1. The solution leaves P_0 at $\tau = \tau_0$, goes through the domain D, where the diode pair is off, and hits the plane D^+ on P_1 at $\tau = \tau_1$, when the diode pair is $+on$. The solution moves constrained by the plane D^+ and hits again the curved line C^+ on P_2 at $\tau = \tau_2$.

2. The solution leaves P_0 at $\tau = \tau_0$, goes through the domain D, where the diode pair is off, and hits the plane D^- on P_1 at $\tau = \tau_1$, when the diode pair is $-on$. The solution moves constrained by the plane D^- and hits the curved line C^- on P_2 at $\tau = \tau_2$.

Because the system is invariant against the transformation $(\tau, x, \dot{x}) \to (\tau + 2\pi/\omega, -x, -\dot{x})$, the solutions whose initial points are on the line C^- are classified similarly. Therefore the Poincaré map T can be defined as the following one-dimensional map.

$$T : (C^+ \cup C^-) \to (C^+ \cup C^-), \ \theta \mapsto T(\theta),$$

$$\theta = \begin{cases} \omega\tau_0/2\pi \bmod 1, & \text{for } P_0 \in C^+, \\ (\omega\tau_0/2\pi \bmod 1) + 1, & \text{for } P_0 \in C^-, \end{cases}$$

$$T(\theta) = \begin{cases} \omega\tau_2/2\pi \bmod 1, & \text{for } P_2 \in C^+, \\ (\omega\tau_2/2\pi \bmod 1) + 1, & \text{for } P_2 \in C^-. \end{cases} \quad (7)$$

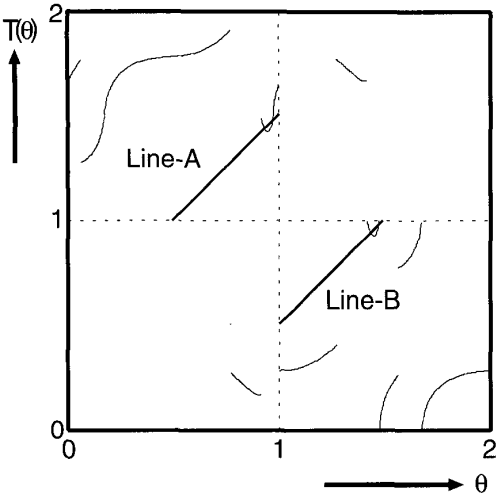

Figure 4: Poincaré map.

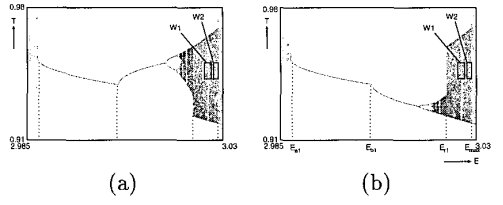

(a) (b)

Figure 5: Bifurcation diagram.

The derivation of the Poincaré map T is omitted. In Fig. 4, an example of the Poincaré map is shown.

4. TWO TYPES OF WINDOWS

In the following discussions, a parameter E is varied and (ω, δ) is fixed to (0.3, 0.29). Fig. 5 shows a one-parameter bifurcation diagram obtained from the Poincaré map T. Let $\theta_n = T^n(\theta_0)$. In Fig. 5, $\theta_{500} ... \theta_{1000}$ are plotted. Note that different initial values are used between Fig. 5 (a) and (b). The initial values are explained below.

Now detailed explanation for bifurcation phenomena observed in Fig. 5 is given by analyzing the Poincaré map in the following. Because Eq. (2) is invariant against the transformation $(\tau, x, \dot{x}) \rightarrow (\tau + 2\pi/\omega, -x, -\dot{x})$, the following holds.

$$T(\theta + 1 \bmod 2) \bmod 1 = \begin{cases} T(\theta + \frac{1}{2} \bmod 1) \bmod 1, & \text{for } 0 \le \theta < 1, \\ T\{(\theta + \frac{1}{2} \bmod 1) + 1\} \bmod 1, & \text{for } 1 \le \theta < 2. \end{cases} \quad (8)$$

Let us draw auxiliary lines Line-A and Line-B as shown in Fig. 4. Line-A is $T(\theta) = \theta + 0.5$ and Line-B is $T(\theta) = \theta - 0.5$. Fig. 6 is a enlarged picture which shows the neighborhood of the intersections

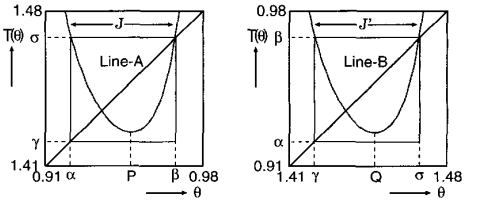

(a) (b)

Figure 6: Enlarged picture of Poincaré map.

of the auxiliary lines and the Poincaré map. Now we introduce some symbols. Let P and Q denote the values of θ that take the extremal values in the sections shown in Fig. 6 (a) and (b) respectively. They are used as the initial values to obtain Fig. 5 (a) and (b) respectively. Let β denote the value of θ at an intersection of Line-A and the Poincaré map as shown in Fig. 6 (a). $\alpha (\neq \beta)$ denotes the values of θ which satisfies $T(\alpha) = T(\beta)$. The section J is defined as follows.

$$J = [\alpha, \beta]. \quad (9)$$

Shown in Fig. 6 (b), σ, γ, and J' are defined similarly. Considering Eq. (8), the following equations hold.

$$\gamma = \left(\left(\alpha + \frac{1}{2} \right) \bmod 1 \right) + 1,$$
$$\sigma = \left(\left(\beta + \frac{1}{2} \right) \bmod 1 \right) + 1,$$
$$\alpha = \left(\gamma - \frac{1}{2} \right) \bmod 1, \quad \beta = \left(\sigma - \frac{1}{2} \right) \bmod 1. \quad (10)$$

Furthermore, it is evident from Eq. (8) that the sections J and J' of the Poincaré map are the same in shape. In the neighborhood of the parameter value at which Fig. 6 is given,

$$\gamma \le T(P) \le \sigma. \quad (11)$$

Therefore

$$T(J) \subset J'. \quad (12)$$

Similarly

$$T(J') \subset J. \quad (13)$$

Thus $T^2(J) \subset J$ and $T^2(J') \subset J'$. It follows that windows appear on J in the neighborhood of this parameter value. Fig. 7 shows the map T when $E = E_{a1} = 2.987$ and when $E = E_{max} = 3.029$. T touches Line-A and Line-B when $E = E_{a1}$. $T(P) = \gamma$ and $T(Q) = \alpha$ when $E = E_{max}$. $T^2(J) \subset J$ and $T^2(J') \subset J'$ holds while $E_{a1} < E < E_{max}$.

A tangent bifurcation occurs when $E = E_{a1}$. The shape of the composite map T^2 is shown by A in Fig. 8 (a). There exists a stable fixed point as illustrated with B in Fig. 8 (a), while $E_{a1} < E < E_{b1}$. At that time, the shape of an attractor is symmetric

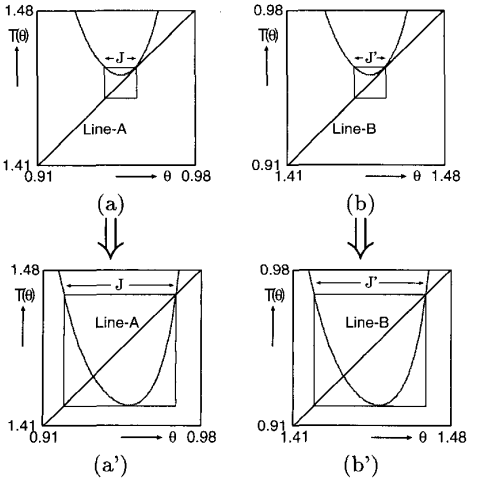

Figure 7: Enlarged picture of Poincaré map. (a)(b) $E = E_{a1} = 2.987$. (a')(b') $E = E_{max} = 3.029$.

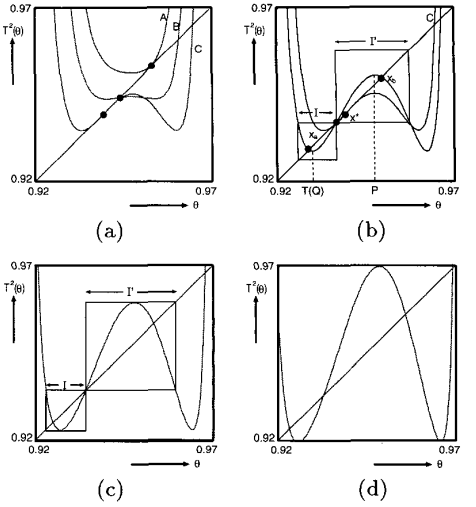

Figure 8: Composite map T^2. (a) A: $E = E_{a1}$. B: $E_{a1} \leq E < E_{b1}$. C: $E = E_{b1}$. (b) $E_{b1} \leq E < E_{r1}$. (c) $E = E_{r1}$. (d) $E = E_{max}$.

with respect to the origin in the phase space of the governing equation.

A symmetry breaking bifurcation occurs when $E = E_{b1}$. The fixed point becomes unstable as shown by x^* in Fig. 8 (b). Illustrated with x_a and x_b in Fig. 8 (b), two stable fixed points appear. At that time, the shapes of attractors are unsymmetric with respect to the origin. Varying the value of a parameter, chaos appears by the route of period doubling bifurcation.

A symmetry recovering crisis[1] occurs when $E = E_{r1}$. The extremal values of the map T^2 go outside the sections I and I' as shown in Fig. 8 (c). The unsymmetric chaotic attractor bifurcates into the chaotic attractor whose shape is symmetric with respect to the origin.

An interior crisis[1] occurs when $E = E_{max}$. The extremal values of the map T^2 go outside the section J as shown in Fig. 8 (d). There disappears the chaotic attractor which existed while $E_{r1} < E < E_{max}$.

It has been proved[1] that a countably infinite number of certain two types of windows are generated alternately, if the shape of the map in the section J is like a parabola, if there exists the case in which the map touches Line-A and Line-B as shown in Fig. 7 (a) and (b), and if there exists the case in which the extremal values of the map hit the end point of the section as shown in Fig. 7 (a') and (b'). Thus, in the non-autonomous circuit proposed in the present study, it is clarified that a countably infinite number of certain two types of windows are generated alternately. In fact, the two types of windows are observed as shown in Fig. 9. One type is a window in which symmetry breaking bifurcation occurs, and which is called Type 1. The other is a window where the shape of the attractor stays unsymmetric with respect to the origin, and which is called Type2.

Fig. 9 (a) and (b) are enlarged pictures which show W_1 in Fig. 5. Fig. 9(c) and (d) are enlarged pictures which show W_2 in Fig. 5. Note that different initial values are used between Fig. 9 (a) and (b). And also between (c) and (d).

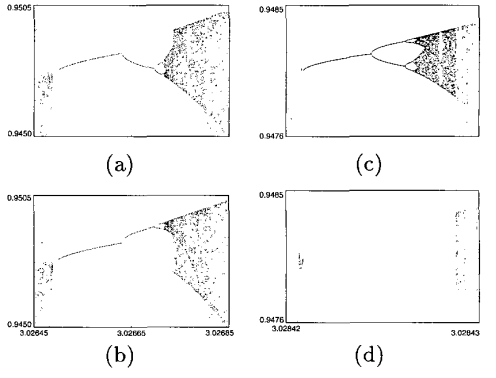

Figure 9: Windows. (a)(b) Type 1. (c)(d) Type 2.

5. REFERENCES

[1] Y. Nishio, N. Inaba, S. Mori, and T. Saito, "Rigorous analyses of windows in a symmetric circuit," IEEE Trans. Circuits Syst., vol. 37, no. 4, pp. 473-487, April, 1990.

[2] L. O. Chua, M. Komuro, and T. Matsumoto, "The double scroll family," IEEE Trans. Circuits Syst., vol. CAS-33, pp. 1072-1118, Nov., 1986.